Geophysical Research Letters

RESEARCH LETTER
10.1029/2019GL083021

# A Subannual Subsurface Pathway From the Gulf Stream to the Subpolar Gyre and Its Role in Warming and Salinification in the 1990s

**Zoe L. Jacobs[1], Jeremy P. Grist[1], Robert Marsh[2], and Simon A. Josey[1]**

[1]National Oceanography Centre, University of Southampton, Southampton, UK, [2]Ocean and Earth Science, University of Southampton, Southampton, UK

**Key Points:**
- Rapid (<1 year) subsurface pathway from Gulf Stream to subpolar gyre is identified for the first time using targeted particle tracking
- Pathway is most evident for particles initially at 200-m depth and is enhanced after a positive phase of the North Atlantic Oscillation
- Western subpolar gyre warming and salinification since the 1990s attributed to anomalous advection via the new pathway

**Supporting Information:**
- Supporting Information S1
- Figure S1
- Figure S2
- Figure S3

**Correspondence to:**
Z. L. Jacobs,
zoe.jacobs@noc.ac.uk

**Citation:**
Jacobs, Z. L., Grist, J. P., Marsh, R., & Josey, S. A. (2019). A subannual subsurface pathway from the Gulf Stream to the Subpolar Gyre and its role in warming and salinification in the 1990s. *Geophysical Research Letters*, *46*, 7518–7526. https://doi.org/10.1029/2019GL083021

Received 26 MAR 2019
Accepted 17 JUN 2019
Accepted article online 24 JUN 2019
Published online 6 JUL 2019



**Abstract** The transport of warm, saline subtropical water to the subpolar gyre (SPG) in the North Atlantic has been the subject of a range of Lagrangian studies, establishing intergyre exchange on timescales of 2–7 years, with greater subsurface throughflow. Here calculating particle trajectories in a high-resolution, global hindcast, we present new evidence for a direct, subsurface pathway to the SPG from the Gulf Stream (GS) on subannual timescales. The pathway is most evident for particles initially at 200-m depth in the GS and is enhanced after a prolonged period of positive North Atlantic Oscillation. This occurred in the mid-1990s and led to warming and salinification of the western SPG consistent with observations. The more realistic advective pathways and timescales in the high-resolution model enable, for the first time, attribution of temperature and salinity changes in the SPG to a direct influx of GS water.

**Plain Language Summary** The downstream destination of Gulf Stream water is investigated using a technique that tracks water parcels with a state-of-the-art ocean model. This approach allows us to obtain new evidence for a fast pathway by which water starting in the Florida Straits at the subsurface (at about 200 m deep) can reach the subpolar North Atlantic on timescales as short as 4 months. Surface waters were more likely to be recirculated within the subtropical region. The subsurface pathway was found to be enhanced during the 1990s, which led to increased temperature and salinity in the western subpolar North Atlantic, in agreement with observations made at this time. Our results have physical and biological implications and indicate that the connection between the subtropical and subpolar North Atlantic on subannual timescales is a key element of the Atlantic climate system.

## 1. Introduction

Pathways between the North Atlantic subtropical gyre (STG) and subpolar gyre (SPG) have been the subject of a wide range of observation and model-based studies (e.g., Brambilla & Talley, 2006; Burkholder & Lozier, 2011; Burkholder & Lozier, 2014; Foukal & Lozier, 2016; Hakkinen & Rhines, 2009; Rypina et al., 2011). Within an Eulerian framework, about 20 Sv of Gulf Stream (GS) water continues as the North Atlantic Current (NAC; Johns et al., 1995). However, this has been disputed by observational and modeling Lagrangian studies that show few surface trajectories from the STG reaching the SPG (e.g., Brambilla & Talley, 2006; Foukal & Lozier, 2016). Brambilla and Talley (2006) found only 1 of 273 surface drifters flowing through a near-GS box during 1992–2002 reached the Nordic Seas. In a recent study, less than 0.01% of modeled surface trajectories were able to cross 53°N after 5 years (Foukal & Lozier, 2016).

Greater intergyre exchange has been found in subsurface pathways beneath the climatological mixed layer (Burkholder & Lozier, 2014; Foukal & Lozier, 2016) with an optimum depth in the STG interior of 700 m (Burkholder & Lozier, 2011). The apparent surface layer "barrier" is thought to be due to a combination of factors including southward Ekman transport (Brambilla & Talley, 2006) and a strong potential vorticity gradient across the GS core, associated with a large horizontal density gradient (Bower et al., 1985). These factors weaken with depth, enabling more intergyre exchange than at the surface but on relatively long timescales of up to 7 years when tracer particles are released in the STG interior (e.g., Burkholder & Lozier, 2011). Rypina et al. (2011) found that this timescale can be reduced to within 2 years for surface particles released in the main GS core, which suggests that at the subsurface, a more direct pathway may exist.

Here we present novel evidence for a subannual (4 months to 1 year) subsurface pathway from the GS to the SPG. Our experiment design is distinct from other studies in that all particles are released in the GS before it

separates from the coast. This approach samples the direct and rapid intergyre pathway. We also show that positive North Atlantic Oscillation (NAO) conditions led to an enhancement of this pathway, enabling the transport of an anomalously large amount of subtropical waters northward to the SPG from the late 80s to the late 90s. The highest rate of throughput occurred to the western SPG via a deeper than normal pathway (see below), leading to positive temperature and salinity anomalies in the region.

In section 2, the model hindcast and Lagrangian methods are described. The main results are presented in section 3 including identification of rapid GS pathways at different depths (section 3.1), interannual variability of the throughput to the SPG (section 3.2), and interdecadal variability of the properties of water reaching the SPG between the 1990s and 2000s. Section 4 provides a summary and conclusions.

## 2. Materials and Methods

### 2.1. Nucleus for European Modelling of the Ocean Model

This study utilizes a global ocean hindcast spanning 1978–2010, with the eddy-resolving ORCA12 configuration of the ocean model Nucleus for European Modelling of the Ocean (Madec, 2015), which is initialized from rest using the World Ocean Atlas 2005 climatological fields (Antonov et al., 2006; Locarnini et al., 2006). The ORCA12 configuration comprises horizontal resolution of (1/12)° and 75 vertical levels, with finer near-surface grid spacing. Surface forcing is provided by the DFS4.1 data set (see Blaker et al., 2015, and references therein), which includes monthly mean precipitation and 6-hourly means of 2-m air temperature/humidity and 10-m wind velocity. With high fidelity in surface forcing and high spatial resolution, the hindcast compares favorably with observations, that is, surface currents, sea surface temperature, eddy activity, and GS position (Marzocchi et al., 2015). Realistic advective timescales and dispersion are associated with well-resolved boundary and inertial currents, and realistic eddy statistics, in ORCA12 (Blaker et al., 2015; Marzocchi et al., 2015; Moat et al., 2016).

Model results are compared with the observational data set EN4 (Good et al., 2013) in section 3.3. Original data sources of EN4 include the World Ocean Database (WOD; Boyer et al., 2009), the Global Temperature–Salinity Profile Programme (from 1990), and Argo profiling floats. After undergoing quality control, the data are objectively analyzed onto a 1° grid with 42 vertical levels for each month from 1900 to the present (see Good et al., 2013 for details).

### 2.2. Lagrangian Experiments

The hindcast provides input data for particle tracking calculations, using Ariane, an offline mass-preserving Lagrangian scheme (Blanke & Raynaud, 1997). Experiments are run using multiple point particle releases into the 5-day mean velocity fields of ORCA12 (e.g., Popova et al., 2013). Particle trajectories are subject to 5-day updates of the velocity field, a "stepwise stationary" scheme (Döös et al., 2017). While a higher temporal resolution may capture the eddy variability more fully, 5-day means are in line with CMIP6/OMIP protocol (Griffies et al., 2016). Time interpolation of the 5-day averages would potentially reduce errors in particle trajectories; this interpolation is not implemented in Ariane, but such errors are limited by our use of a large ensemble as shown by Döös et al. (2017). The advected particles characterize and quantify selected features of the ocean circulation from a Lagrangian perspective, recording water mass properties along trajectories.

A total of 30 experiments were performed, one for each year from 1980–2009 (avoiding potential spin up issues in the first few years), with particles released at the beginning of each month throughout each year (12 releases per year) and at five different depths to sample the upper water column: 10, 50, 100, 200, and 300 m resulting in a total of 60 releases per experiment (supporting information Figure S1). Each "annual" experiment is run for a total of 2 years to ensure that every monthly release has a minimum run time of 1 year, that is, January releases run for 2 years and December releases for 13 months. Starting in the core of the GS, while ensuring that we sample eddy variability, 400 particles are initiated in a single ~10-km grid box (where they are uniformly distributed in longitude and latitude) in the Florida Straits at 26°N, 80°W, for each individual release (i.e., per month and per release depth, which results in $400 \times 12 \times 5$ particles per experiment). This experimental design is distinct from other studies in that the release location has been chosen such that all particles directly enter the GS before separation from the coast around Cape Hatteras.

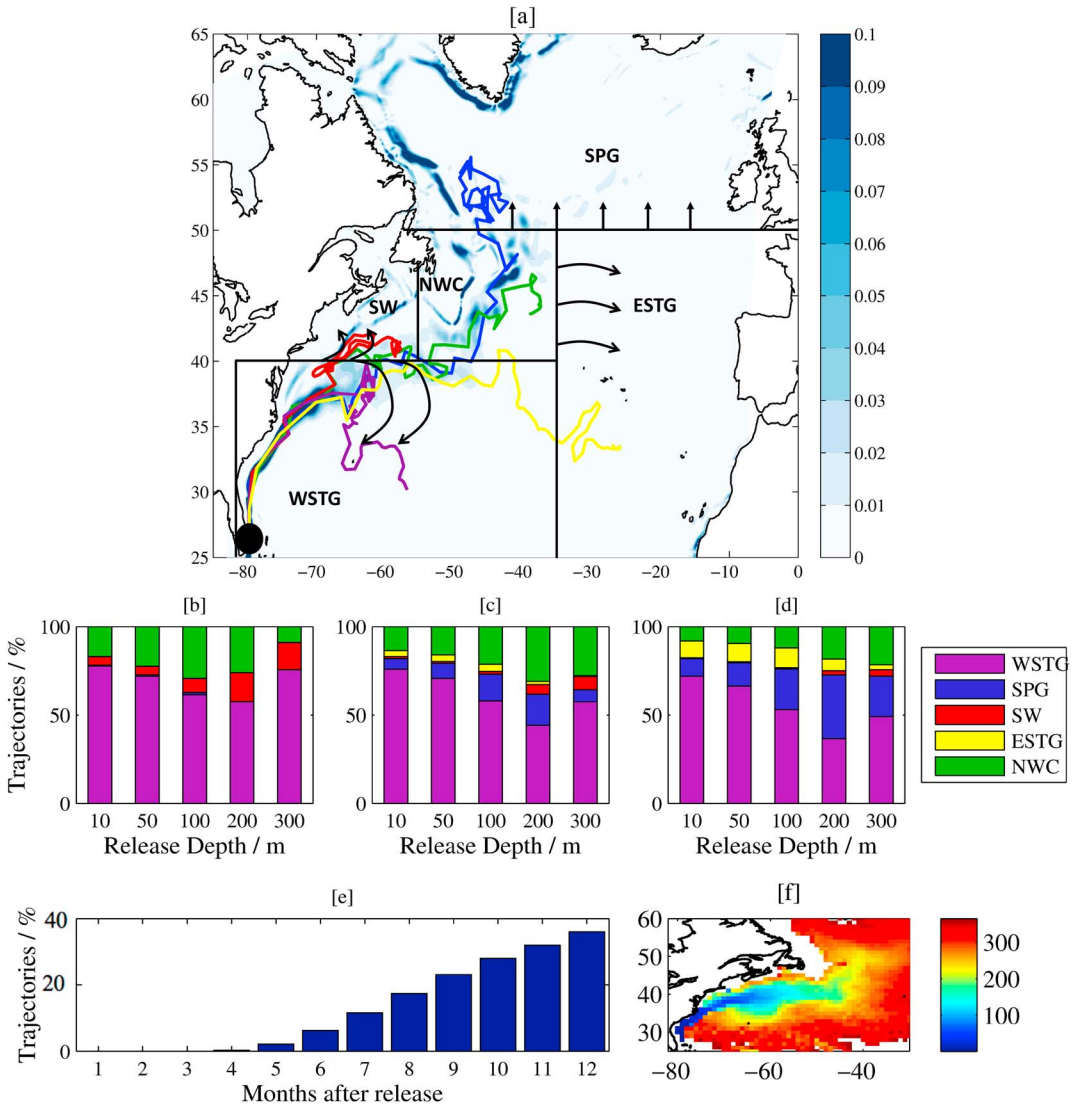


**Figure 1.** (a) Mean surface currents (m/s) from 1980–2010 in the ORCA12 hindcast, with the following regions defined: the subpolar gyre (SPG), the western Subtropical Gyre (WSTG), the eastern Subtropical Gyre (ESTG), the Slope Water (SW), and the Northwest Corner (NWC), with example trajectories in each region; the black marker represents the release location in the Florida Straits. Downstream destination of particles released at 26°N, 80°W (by percentage of total particles released at a given depth level) after (b) 4 months, (c) 8 months, and (d) 1 year when averaged over all release months and years. (e) The average percentage of particles reaching the SPG at 200 m for 1–12 months after release. (f) The mean age (days) of particles released at 200 m.

The GS water can continue northeast as the NAC into the SPG, east as the Azores Current, or recirculate to the south or to the north (Schmitz, 1996). In order to quantify the variability in its downstream destination, we define five regions into which the GS water has entered via one of the main pathways after bifurcation. These are the Northwest Corner (NWC), SPG, eastern STG, the Slope Water (SW), and the western STG (WSTG; see Figure 1a). Particles entering the SPG via the NAC are defined as crossing 50°N, those in the WSTG as being south of 40°N and west of 35°W, and those in the SW as north of 40°N and west of 55°W, while those that have continued east in the Azores Current have entered the wider eastern STG recirculation, south of 50°N and east of 35°W.

## 3. Results

### 3.1. Depth Dependence of Pathway

Variability of GS pathways with depth and time is evident in Figure 1, which shows the average percentage of particles in each of the defined regions, for each depth after 4 months (Figure 1b), 8 months (Figure 1c),

and 1 year (Figure 1d). Figure 1e reveals the average percentage of particles residing in the SPG after 1–12 months for subsurface (200 m) trajectories, and Figure 1f shows the distribution of mean particle age across all 200-m release experiments.

After 4 months, considering all depths, less than 1% of particles have crossed the boundary into the SPG. The majority (55–76%, depending on depth) remain in the WSTG, but a substantial percentage (5–15%) are already in the SW and in the NWC (10–25%). As release depth increases to 200 m, fewer particles remain in the WSTG and more are in the SW or the NWC. After 8 months, a significant proportion of the particles make it to the SPG, with increased throughflow at greater depths (6% at 10 m and 17% at 200 m). By 300 m, there is a slight reversal in this trend, likely due to a reduced current speed at this depth.

After 1 year, 72% of particles released at 10 m reside in the WSTG, which identifies it as the most favorable GS pathway at this release depth. This value decreases to 55% at 200 m and is compensated by a greater proportion of particles traveling to the SPG via the NAC pathway. For the 200-m release, 36% of all particles reach the SPG after 1 year, while this value is less than 10% when released near the surface (10 m). However, this may be underestimated as the particles are released slightly eastward of the main GS core (supporting information Figure S1). This implies that subsurface trajectories, that is, those residing on a denser isopycnal, are more likely to reach the SPG, which agrees with previous findings (e.g., Burkholder & Lozier, 2011; Foukal & Lozier, 2016). However, these studies are associated with longer timescales (4–5 years) to enable eventual entrainment into the GS when released in the WSTG. Here we determine, for the first time, the timescale of the direct GS pathway (less than 1 year). This is highlighted in Figure 1e, which shows the gradual progression of particles reaching the SPG from 4–12 months via the direct subsurface pathway. This value increases to about 50% by 16–17 months where it stabilizes until 24 months, shown for January releases in supporting information Figure S3.

At all time periods up to 1 year, most particles reside in either the WSTG or the SPG, which implies that these are the two main GS pathways at all depths. We note here that the WSTG will include particles that remain in the main GS, but this will only affect the results in the first month or so as shown by the mean particle age in Figure 1f.

To summarize, our results indicate a depth dependence of the GS to SPG pathway, with greatest throughflow efficiency at 200 m. They provide the first evidence for a direct subsurface pathway between the GS and the SPG on timescales as short as 4 months. The identification of a subsurface pathway on such short timescales builds on prior findings that were concerned with routes from the STG interior (Burkholder & Lozier, 2011; Burkholder & Lozier, 2014; Foukal & Lozier, 2016). For example, Burkholder and Lozier (2011) found a timescale for particles reaching the SPG of 2- to 7-year timescales when released in the STG interior at 700 m. Our results indicate an additional "window" of interconnectivity such that some STG water can reach the SPG on much shorter timescales than has been found in previous Lagrangian model studies with timescale depending on proximity to the GS.

### 3.2. Interannual to Interdecadal Variability of Subsurface Pathway

The interannual variability of the 200-m subsurface pathway to the SPG for each month is evident in Figure 2a, which shows the percentage of trajectories reaching the SPG. A steady increase is evident from the 1980s to the mid-1990s, followed by a decline until 2009. This is potentially related to evolution of the winter NAO, which is displayed in Figure 2b alongside the winter (December–February [DJF]) average throughput to the SPG. The positive NAO phase dominates the late 1980s until 1995 and is followed by a more neutral period that was punctuated with several sharp NAO negative years (e.g., in 1996 and 2010). The percentage of DJF-release trajectories reaching the SPG is significantly correlated, to the 95% confidence interval (assessed by calculating the effective number of degrees of freedom from Bretherton et al., 1999) with the NAO index at a 2-year lag ($r = 0.48$). This indicates that the surge of GS waters into the SPG in the early 1990s may be a response to the persistently positive phase of the NAO in much of the 1980s. However, the NAO affects many aspects of the ocean circulation (see details below), so the specific mechanisms controlling this relationship are complex and should be the focus of future studies.

Several previous studies have addressed how the NAO influences the SPG with clear distinctions between the eastern and western halves (e.g., Herbaut & Houssais, 2009; Robson, Sutton, Lohmann, et al., 2012; Sarafanov, 2009). Having established a direct pathway that influences the western half of the SPG, that is

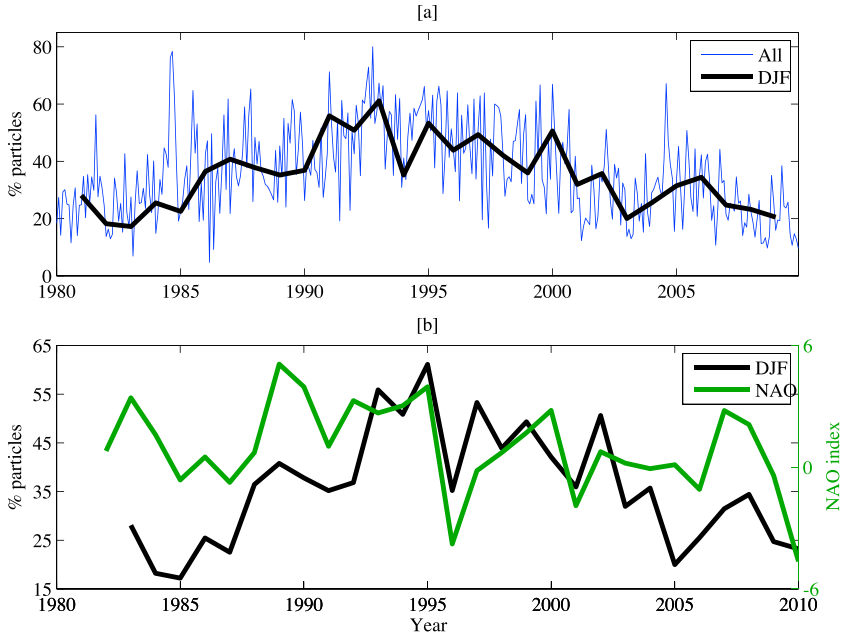


**Figure 2.** (a) Percentage of 200-m particles in the subpolar gyre after 1 year for releases in each individual month (all; blue line) and releases averaged over winter months (December–February [DJF], black line). (b) The winter average (black) replotted alongside the winter North Atlantic Oscillation (NAO) index (green, determined from the difference of normalized sea level pressure between Lisbon and Reykjavik) with DJF lagged by 2 years.

our regional focus here. During positive NAO winters such as 1988–1995, there was a greater heat loss over the Labrador Sea due to strengthened Westerlies, which intensified deep convection and lead to a greater formation of Labrador Sea Water (Hurrell et al., 2003). This caused anomalously cold and fresh anomalies to prevail at intermediate levels in the western SPG (Sarafanov, 2009). However, after prolonged periods of positive NAO the increased deep water formation leads to an intensification of the Atlantic meridional overturning circulation (AMOC; Dong & Sutton, 2005; De Coëtlogon et al., 2006; Eden & Willebrand, 2001; Lohmann et al., 2009; Robson, Sutton, Lohmann, et al., 2012). These AMOC changes are seen in reanalyses and models (Böning et al., 2006; Grist et al., 2010) and lead to an anomalously warm western SPG (Robson, Sutton, Lohmann, et al., 2012). We note here that the mid-1990s AMOC spin up is consistent with our results of increased particle through flow to the SPG (Marzocchi et al., 2015).

In Figure 3, we present statistics for the average (200 m) pathways of trajectories traveling to the SPG during the periods 1992–1999 and 2000–2007, hereby referred to as the 1990s and 2000s, which represent periods of increased and decreased flow to the SPG, respectively. Figures 3a and 3b reveal very little difference in the average latitude between the two periods. During the 1990s, the pathway was slightly further north from about 140–250 days, but this is likely due to a shorter transit time compared with the 2000s. However, there is evidence that the GS is in a more northward position during the 1990s, from about 80–70°W (supporting information Figure S2), which may have encouraged a greater proportion of trajectories to take the SPG pathway.

When there is a greater through flow to the SPG during the 1990s, the trajectories follow a deeper pathway after about 25 days with trajectories arriving up to 40 m deeper, on average, than in the 2000s (Figure 3c). Overall, during the 1990s, more trajectories remained at greater depth, and therefore on a denser isopycnal, after separation from the coast at Cape Hatteras, which favored increased flow to the SPG. This is confirmed in Figure 3d, which shows that trajectories follow a denser (by up to 0.2 kg/m$^3$) pathway during the 1990s. From 25–200 days, the mean pathway is cooler by up to 1 °C (Figure 3e). However, the temperature during the two periods is comparable after day 200. In contrast, the salinity prior to 150 days is similar during both periods but then begins to diverge, with a more saline path during the 1990s (Figure 3f).

The difference in trajectory density is likely due to competing effects of temperature and salinity with temperature being dominant from 25–150 days and salinity dominating thereafter. Figure 3d reveals that the

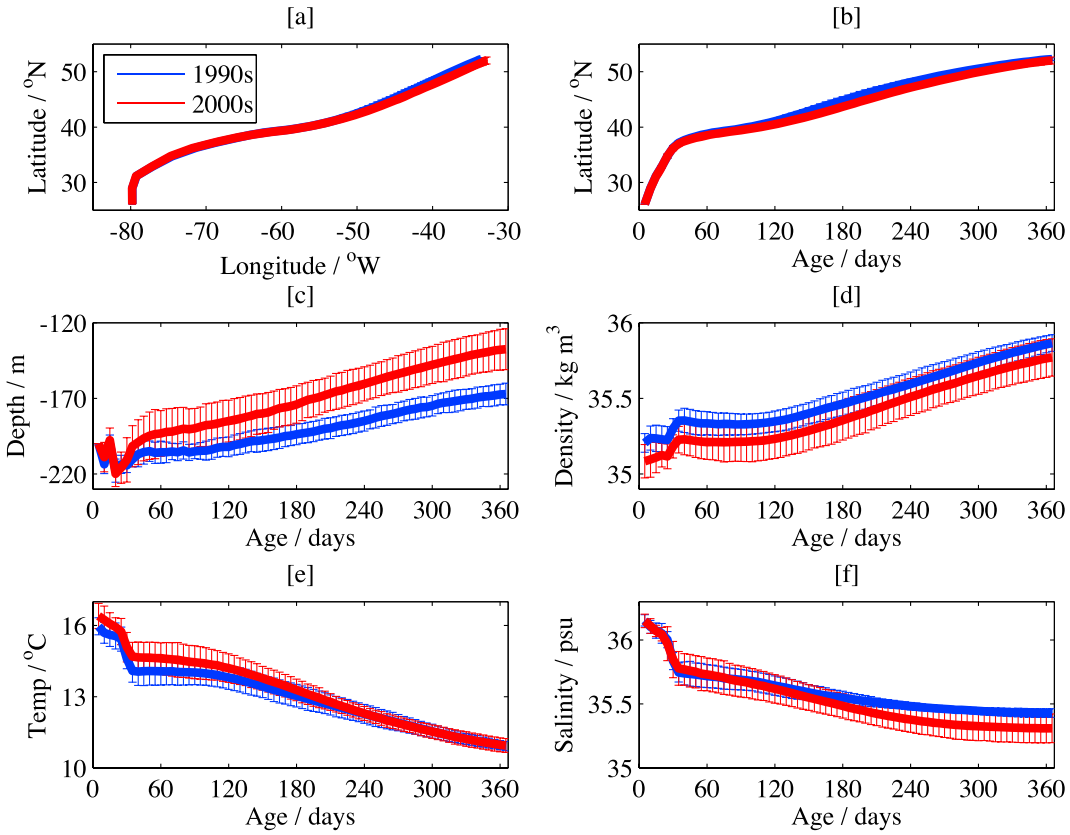


**Figure 3.** Variation in trajectory properties after 1 year for particles initially released at 200 m in the Florida Straits. (a) Average latitude (°N) with average longitude (°W), (b) average latitude (°N) with age (days), (c) depth (m) with age, (d) density (kg/m$^3$) with age, (e) temperature (°C) with age, and (f) salinity with age. Red: particles released from 1992–1999 (referred to as 1990s) and blue: 2000–2007 (referred to as 2000s). Error bars are the standard deviation of the annual average at each 5-day interval.

trajectories released in the 1990s begin on a denser isopycnal when released in the Florida Straits. This could also explain the greater throughput to the SPG during this decade with trajectories residing on a denser isopycnal more likely to reach the northward side of the GS and travel directly to the SPG, where they continue to cool and increase their density.

### 3.3. Warming and Salinification of the Western SPG

An example of contrasting monthly trajectory maps, October 1992 and 2009, is displayed in Figure 4a. These releases were selected as they are from the years that exhibit the greatest and least throughput to the SPG, respectively. In 1992 (red), trajectories extend further into the SPG in all directions, compared to the trajectories for 2009 (blue), but most notably in the western SPG.

To quantify these differences, a trajectory density is obtained by spatially averaging the number of trajectories passing through each grid cell on a 1° grid. This is time averaged over the high throughput period (1990s) and the low throughput period (2000s) with the difference taken between them (high-low) to give a composite difference. This is shown in Figure 4b, which reveals a positive anomaly in much of the area north of 45°N. In contrast, a negative anomaly exists over much of the STG, notably to the immediate south of the GS core. This provides further evidence that during the 1990s, more subsurface GS trajectories travel north in the NAC as opposed to recirculating in the STG. Specifically, up to 200 more particles per grid cell flow into the western SPG during the earlier period with the greatest anomalies evident in the western SPG region spanning 50–55°N, 45–35°W.

Figure 4c shows that the trajectories in the western SPG were up to 1 °C warmer in the 1990s. This contrasts with evidence in Figure 3e for similar average temperature for the two periods after about 200 days. However, this is averaged across the entire SPG where the warm anomalies in the west are

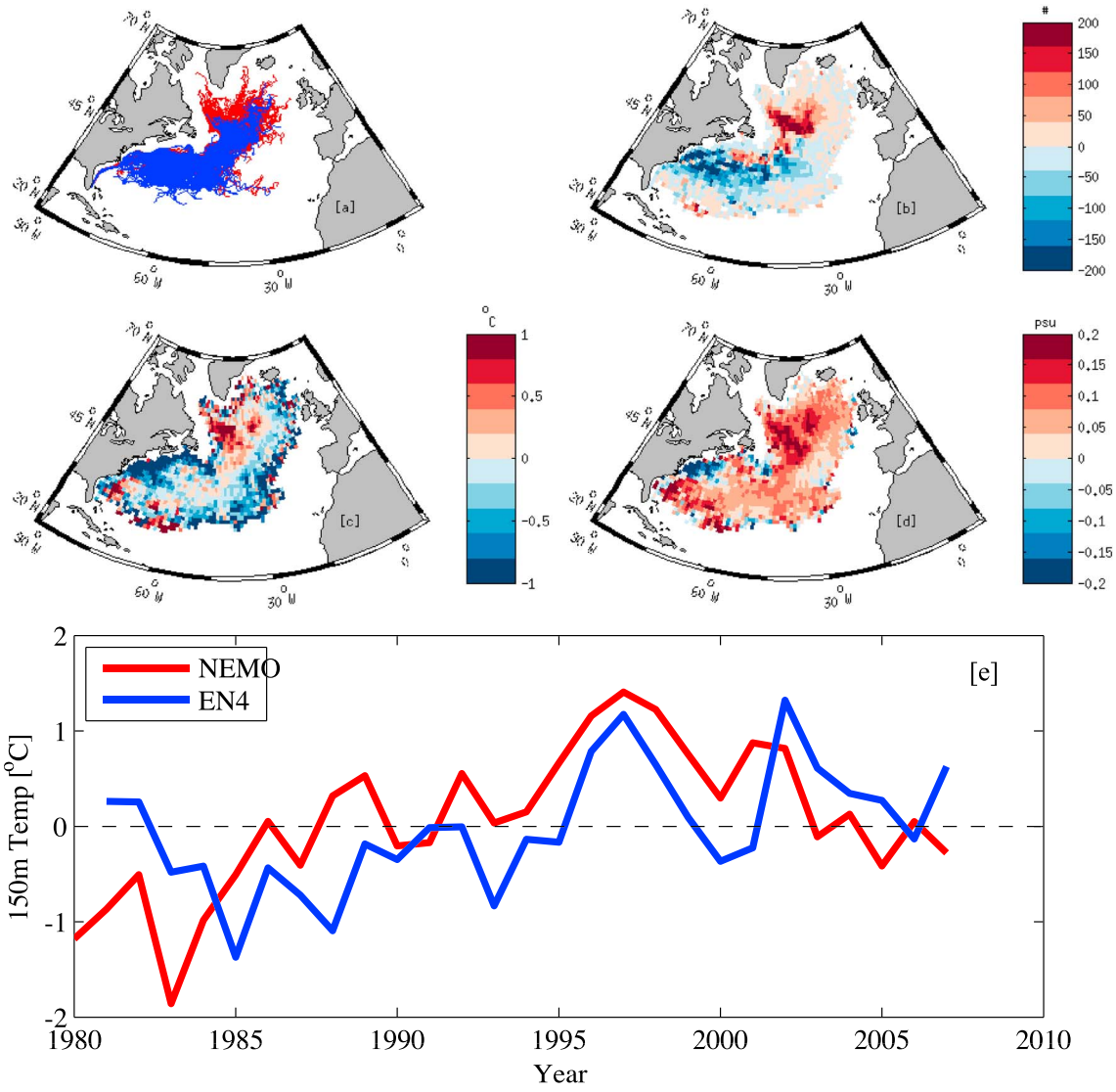


**Figure 4.** (a) Trajectories of particles released at 200 m in October 1992 (red) and 2009 (blue), (b) composite anomaly difference (1992–1999 minus 2000–2007) for trajectory density (number of particles per 1° grid box), (c) as (b) for temperature (°C), and (d) as (b) for salinity (psu). All particles have been allowed to travel in the flow field for 1 year. (e) winter (December–February) subsurface temperature anomalies at 150 m in the western Subtropical Gyre (50–55°N, 45–35°W) in ORCA12 (red) and the observational product EN4 (blue). Note that 150 m is chosen to match the mean depth of trajectories in the subpolar gyre after 1 year (see Figure 3c). NEMO = Nucleus for European Modelling of the Ocean.

counterbalanced by cold anomalies in the east. Additionally, Figure 4d shows anomalously saline waters, up to 0.2 psu, exist over much of the North Atlantic during the earlier period. However, the western SPG exhibits a greater anomaly compared to the rest of the SPG. This implies that the anomalously warm and saline waters seen in this region are a consequence of the greater influx of GS waters.

Figure 4e shows time series of 150-m temperature over the western SPG in the model as well as the observational product EN4. Both indicate the warming occurring between the mid-1980s to the mid-1990s, with a peak warm anomaly (>1 °C) occurring in the same year (1997). The 150-m temperature time series closely follows the percentage of trajectories traveling to the SPG (Figure 2a) but with a lag of 2 years ($r = 0.67$). This result builds on prior studies that found that an increased meridional heat transport, as opposed to surface heat fluxes, was responsible for the SPG warming in the mid-1990s (e.g., Robson, Sutton, Lohmann, et al., 2012; Yeager et al., 2012). Here we provide evidence for the first time that this warming was conveyed to the SPG via a direct subsurface GS pathway. Additionally, the warming found here occurred at the same time as observations, which is faster than in previous studies with models of coarser horizontal resolution

(e.g., Robson, Sutton, & Smith, 2012; Stepanov & Haines, 2014). The faster response is likely due to the more realistic advective pathways and timescales in ORCA12.

## 4. Conclusions

Here we have used a high-resolution ocean model and particle trajectory calculations to reveal the existence of a rapid subsurface pathway between the GS and the SPG on timescales of less than a year. The identification of a subsurface pathway on such short timescales is a significant development from previous work that focused on routes from the STG interior (e.g., Brambilla & Talley, 2006; Burkholder & Lozier, 2011; Foukal & Lozier, 2016; Rypina et al., 2011). Our results indicate an additional window of interconnectivity and that some STG water can reach the SPG on much shorter timescales than has been found in previous Lagrangian model studies with timescale depending on proximity to the GS. The importance of a fast subtropical-subpolar pathway at 200 m—in contrast to the deeper, slower pathway of Burkholder and Lozier (2011)—is supported by a proposal that "eddy cancellation" of Ekman pumping in STGs may limit particles from downwelling below 200 m (Doddridge et al., 2016).

We also find evidence that this subsurface pathway is enhanced from the mid-80s to the mid-90s, which may have resulted from a period of a sustained positive NAO index and associated changes in the large-scale circulation. However, this relationship is complex as the NAO affects many aspects of the circulation and should be further scrutinized. The anomalously large transport of subtropical waters to the SPG via the GS is in agreement with an observed increase in NAC transport over this period (Curry & McCartney, 2001). This enhanced meridional transport to the SPG can thus be attributed to anomalous subsurface GS flow. A consequence of this enhanced pathway was a warming (up to 1.1 °C) and salinification (up to 0.2 psu) of the western SPG, which was the site of the greatest throughput of particles 1 year after originating in the GS. The pathway was up to 40 m deeper during the period of enhanced throughflow, which enabled the particles to travel on a denser isopycnal.

The consistency between the mid-1990s subsurface warming seen in the model and observations, and its attribution to an increased proportion of GS water reaching the SPG, is of potential importance for the wider circulation. In particular, the advection of heat and salt fluxes to SPG will likely influence subsequent deep convection and, consequently, the strength of the AMOC. As well as the physical consequences there are potential biological implications as warming of the western SPG may impact temperature-sensitive species such as Atlantic cod (Drinkwater, 2005). Our results strongly indicate that subtropical-subpolar connectivity on subannual timescales is a key element of the Atlantic climate system that needs to be resolved in ocean and climate forecast systems.

**Acknowledgments**

Z. J. was supported by a studentship from the Graduate School of the National Oceanography Centre, Southampton. J. G. and S. J. were supported by the UK National Environmental Research Council (NERC) under the ACSIS programme (Ref. NE/N018044/1). R. M. acknowledges funding from several NERC Grants. We acknowledge the use of the UK's national high-performance computing service. The Ariane software was developed by B. Blanke and N. Grima. EN4 grids are from the Met Office (https://http://www.metoffice.gov.uk/hadobs/en4/download-en4-2-0.html)). The model data used for this publication are available from http://gws-access.ceda.ac.uk/public/nemo.

## References

Antonov, J. I., Locarnini, R. A., Boyer, T. P., Mishonov, A. V., Garcia, H. E., & Levitus, S. (2006). World Ocean Atlas 2005, Salinity. *NOAA Atlas NESDIS*, *62*, 2.

Blaker, A. T., Hirschi, J. J. M., McCarthy, G., Sinha, B., Taws, S., Marsh, R., et al. (2015). Historical analogues of the recent extreme minima observed in the Atlantic meridional overturning circulation at 26 N. *Climate Dynamics*, *44*(1-2), 457–473. https://doi.org/10.1007/s00382-014-2274-6

Blanke, B., & Raynaud, S. (1997). Kinematics of the Pacific equatorial undercurrent: An Eulerian and Lagrangian approach from GCM results. *Journal of Physical Oceanography*, *27*(6), 1038–1053. https://doi.org/10.1175/1520-0485(1997)027<1038:KOTPEU>2.0.CO;2

Böning, C. W., Scheinert, M., Dengg, J., Biastoch, A., & Funk, A. (2006). Decadal variability of subpolar gyre transport and its reverberation in the North Atlantic overturning. *Geophysical Research Letters*, *33*, L21S01. https://doi.org/10.1029/2006GL026906

Bower, A. S., Rossby, H. T., & Lillibridge, J. L. (1985). The Gulf Stream—Barrier or blender? *Journal of Physical Oceanography*, *15*(1), 24–32. https://doi.org/10.1175/15200485(1985)015<0024:TGSOB>2.0.CO;2

Boyer, T. P., Antonov, J. I., Baranova, O. K., Garcia, H. E., Johnson, D. R., Mishonov, A. V., et al. (2009). "World ocean database 2009." NOAA Atlas NESDIS66. Washington, DC: U.S. Government Publishing Office.

Brambilla, E., & Talley, L. D. (2006). Surface drifter exchange between the North Atlantic subtropical and subpolar gyres. *Journal of Geophysical Research*, *111*, C07026. https://doi.org/10.1029/2005JC003146

Bretherton, C. S., Widmann, M., Dymnikov, V. P., Wallace, J. M., & Bladé, I. (1999). The effective number of spatial degrees of freedom of a time-varying field. *Journal of Climate*, *12*(7), 1990–2009.

Burkholder, K. C., & Lozier, M. S. (2011). Subtropical to subpolar pathways in the North Atlantic: Deductions from Lagrangian trajectories. *Journal of Geophysical Research*, *116*, C07017. https://doi.org/10.1029/2010JC006697

Burkholder, K. C., & Lozier, M. S. (2014). Tracing the pathways of the upper limb of the North Atlantic Meridional Overturning Circulation. *Geophysical Research Letters*, *41*, 4254–4260. https://doi.org/10.1002/2014GL060226

Curry, R. G., & McCartney, M. S. (2001). Ocean gyre circulation changes associated with the North Atlantic Oscillation. *Journal of Physical Oceanography*, *31*(12), 3374–3400. https://doi.org/10.1175/1520-0485(2001)031<3374:OGCCAW>2.0.CO;2

De Coëtlogon, G., Frankignoul, C., Bentsen, M., Delon, C., Haak, H., Masina, S., & Pardaens, A. (2006). Gulf Stream variability in five oceanic general circulation models. *Journal of Physical Oceanography*, *36*(11), 2119–2135. https://doi.org/10.1175/JPO2963.1

Doddridge, E. W., Marshall, D. P., & Hogg, A. M. (2016). Eddy cancellation of the Ekman cell in subtropical gyres. *Journal of Physical Oceanography*, *46*(10), 2995–3010. https://doi.org/10.1175/JPO-D-16-0097.1

Dong, B., & Sutton, R. T. (2005). Mechanism of interdecadal thermohaline circulation variability in a coupled ocean–atmosphere GCM. *Journal of Climate*, *18*(8), 1117–1135. https://doi.org/10.1175/JCLI3328.1

Döös, K., Jönsson, B., & Kjellsson, J. (2017). Evaluation of oceanic and atmospheric trajectory schemes in the TRACMASS trajectory model v6.0. *Geoscientific Model Development*, *10*, 1733–1749. https://doi.org/10.5194/gmd-10-1733-2017

Drinkwater, K. F. (2005). The response of Atlantic cod (*Gadus morhua*) to future climate change. *ICES Journal of Marine Science*, *62*(7), 1327–1337. https://doi.org/10.1016/j.icesjms.2005.05.015

Eden, C., & Willebrand, J. (2001). Mechanism of interannual to decadal variability of the North Atlantic circulation. *Journal of Climate*, *14*(10), 2266–2280. https://doi.org/10.1175/1520-0442(2001)014<2266:MOITDV>2.0.CO;2

Foukal, N. P., & Lozier, M. S. (2016). No inter-gyre pathway for sea-surface temperature anomalies in the North Atlantic. *Nature Communications*, *7*(1), 11333. https://doi.org/10.1038/ncomms11333

Good, S. A., Martin, M. J., & Rayner, N. A. (2013). EN4: Quality controlled ocean temperature and salinity profiles and monthly objective analyses with uncertainty estimates. *Journal of Geophysical Research: Oceans*, *118*, 6704–6716. https://doi.org/10.1002/2013JC009067

Griffies, S. M., Danabasoglu, G., Durack, P. J., Adcroft, A. J., Balaji, V., Boning, C. W., et al. (2016). OMIP contribution to CMIP6. *Geoscientific Model Development*, *9*(9), 3231–3296. https://doi.org/10.5194/gmd-9-3231-2016

Grist, J. P., Josey, S. A., Marsh, R., Good, S. A., Coward, A. C., de Cuevas, B. A., et al. (2010). The roles of surface heat flux and ocean heat transport convergence in determining Atlantic Ocean temperature variability. *Ocean Dynamics*, *60*(4), 771–790. https://doi.org/10.1007/s10236-010-0292-4

Hakkinen, S., & Rhines, P. B. (2009). Shifting surface currents in the northern North Atlantic Ocean. *Journal of Geophysical Research*, *114*, C04005. https://doi.org/10.1029/2008JC004883

Herbaut, C., & Houssais, M. N. (2009). Response of the eastern North Atlantic subpolar gyre to the North Atlantic Oscillation. *Geophysical Research Letters*, *36*, L17607. https://doi.org/10.1029/2009GL039090

Hurrell, J. W., Kushnir, Y., Ottersen, G., & Visbeck, M. (2003). An overview of the North Atlantic oscillation. In *The North Atlantic Oscillation: Climatic significance and environmental impact*, *Geophysical Monograph Series*, (Vol. 134, pp. 1–35). https://doi.org/10.1029/134GM01

Johns, W. E., Shay, T. J., Bane, J. M., & Watts, D. R. (1995). Gulf Stream structure, transport, and recirculation near 68 W. *Journal of Geophysical Research*, *100*(C1), 817–838. https://doi.org/10.1029/94JC02497

Locarnini, R. A., Mishonov, A. V., Antonov, J. I., Boyer, T. P., Garcia, H. E., & Levitus, S. (2006). World Ocean Atlas 2005, Temperature. *NOAA Atlas NESDIS*, *61*, 1.

Lohmann, K., Drange, H., & Bentsen, M. (2009). A possible mechanism for the strong weakening of the North Atlantic subpolar gyre in the mid-1990s. *Geophysical Research Letters*, *36*, L15602. https://doi.org/10.1029/2009GL039166

Madec, G. (2015). NEMO ocean engine.

Marzocchi, A., Hirschi, J. J. M., Holliday, N. P., Cunningham, S. A., Blaker, A. T., & Coward, A. C. (2015). The North Atlantic subpolar circulation in an eddy-resolving global ocean model. *Journal of Marine Systems*, *142*, 126–143. https://doi.org/10.1016/j.jmarsys.2014.10.007

Moat, B. I., Josey, S. A., Sinha, B., Blaker, A. T., Smeed, D. A., McCarthy, G., et al. (2016). Major variations in subtropical North Atlantic heat transport at short (5 day) timescales and their causes. *Journal of Geophysical Research: Oceans*, *121*, 3237–3249. https://doi.org/10.1002/2016JC011660

Popova, E. E., Yool, A., Aksenov, Y., & Coward, A. C. (2013). Role of advection in Arctic Ocean lower trophic dynamics: A modeling perspective. *Journal of Geophysical Research: Oceans*, *118*, 1571–1586. https://doi.org/10.1002/jgrc.20126

Robson, J., Sutton, R., Lohmann, K., Smith, D., & Palmer, M. D. (2012). Causes of the rapid warming of the North Atlantic Ocean in the mid-1990s. *Journal of Climate*, *25*(12), 4116–4134. https://doi.org/10.1175/JCLI-D-11-00443.1

Robson, J. I., Sutton, R. T., & Smith, D. M. (2012). Initialized decadal predictions of the rapid warming of the North Atlantic Ocean in the mid 1990s. *Geophysical Research Letters*, *39*, L19713. https://doi.org/10.1029/2012GL053370

Rypina, I. I., Pratt, L. J., & Lozier, M. S. (2011). Near-surface transport pathways in the North Atlantic Ocean: Looking for throughput from the subtropical to the subpolar gyre. *Journal of Physical Oceanography*, *41*(5), 911–925. https://doi.org/10.1175/201JPO4498.1

Sarafanov, A. (2009). On the effect of the North Atlantic Oscillation on temperature and salinity of the subpolar North Atlantic intermediate and deep waters. *ICES Journal of Marine Science*, *66*(7), 1448–1454. https://doi.org/10.1093/icesjms/fsp094

Schmitz, W. J. Jr (1996). On the World Ocean circulation. Volume 1. Some global features/North Atlantic Circulation (No. WHOI-96-03-VOL-1). WOODS HOLE OCEANOGRAPHIC INSTITUTION MA.

Stepanov, V., & Haines, K. (2014). Mechanisms for AMOC variability simulated by the NEMO model. *Ocean Science*, *10*(4), 645–656. https://doi.org/10.5194/os-10-645-2014

Yeager, S., Karspeck, A., Danabasoglu, G., Tribbia, J., & Teng, H. (2012). A decadal prediction case study: Late twentieth-century North Atlantic Ocean heat content. *Journal of Climate*, *25*(15), 5173–5189. https://doi.org/10.1175/JCLI-D-11-00595.1